SUstainable solutions for affordable REtroFIT of domestic buildings

Call: H2020-LC-SC3-2018-2019-2020

Topic: LC-SC3-EE-1-2018-2019-2020

Type of action: IA

Grant Agreement number	**894511**
Project acronym **Project full title**	**SUREFIT** **SU**stainable solutions for affordable **RE**tro**FIT** of domestic buildings
Due date of deliverable	**30/11/2021**
Lead beneficiary	**SOLIMPEKS**
Other authors	**University of Nottingham (UNOTT)**

WP4 - Deliverable D 4.2

PV vacuum glazing unit

Dissemination Level

PU	Public	**X**
CO	**Confidential, only for members of the consortium (including the Commission Services)**	
CI	Classified, as referred to in Commission Decision 2001/844/EC	

Document History

Version	Date	Authors	Description
1	30/11/2021	SOLIMPEKS and UNOTT	First draft of D4.1
2	01/02/2022	ISQ – Muriel Iten and Ricardo Barbosa	Coordinator review
3	08/04/2022	All partners	Contribution from partners
4	19/04/2022	SOLIMPEKS, UNOTT and ISQ	Final version

This project has received funding from the European Union's Horizon 2020 research and innovation programme under grant agreement No **894511**.

Contents

Table of figures

Table of tables

Abbreviations

PV	Photovoltaic
TVG	Triple Vacuum Glazing
EC	Electrochromic
VG	Vacuum Glazing
SPD	Suspended Particle Device
EVA	Ethylene Vinyl Acetate
RMSPD	Root Mean Square Percentage Deviation

Publishable summary

This report is based on the work that has been published in Journal of Future Cities and Environment, with title of Performance analysis of a hybrid thin film photovoltaic (PV) vacuum glazing. The work discusses a hybrid thin film PV vacuum glazing called: 'PV VG-4L'. The glazing involves an integration between a thin film PV glazing with a double vacuum glazing (both manufactured independently), and an additional layer of self-cleaning coated glass which totalling four layers of glass. The mathematical model of the PV VG-4L designs were developed and numerically solved in MATLAB. To evaluate the performance of the PV VG-4L, the prototype was manufactured and investigated at lab-scale and also under real conditions. Lab-scale experiments were conducted at steady state conditions using a TEC driven calibrated hot box at the Sustainable Energy Research Lab, University of Nottingham, UK. Meanwhile, outdoors, the prototype was tested at a research house at the University of Nottingham, UK. Under the influence of solar irradiance, the electrical performance of the PV-VG and the temperature difference between the surfaces of the glazing were analysed. However, the measurement of U-value under real conditions is not reliable due to the influence of solar irradiance on the heat flux sensor and also due to the absorbed solar irradiance by the thin film PV layer. Nevertheless, during low to zero solar irradiance, the U-value of the prototype can be estimated. The developed model was then validated against the experimental results by direct comparison to the trend of the experimental and theoretical curves obtained, and also by conducting error analysis using root mean squared percentage deviation (RMSPD) method. Testing using the calibrated hot box, adhering closely to ISO 12567 standards, resulted in an average measured total U-value of 0.6 W/m^2K which is when compared to a single thin film PV glazing with a typical U-value of 5 W/m^2K; the U-value is higher by almost 90%. From the analysis, the computed RMSPD value for the glazing surface temperature and the U-value are 4.02% and 0.92% respectively. Meanwhile, field testing under real conditions with a 0.4 m × 0.4 m PV VG-4L prototype found that 14 W/m^2 power can be generated by the PV VG-4L at average solar irradiance of ~600 W/m^2. RMSPD computed glazing surface temperatures, electrical power generated under real conditions and U-value are 2.90%, 8.70% and 2.89% respectively. The theoretical and experimental results are concluded to be in good agreement. This study has significant contributions to the knowledge of building integrated photovoltaic PV technology. The mathematical model that has been developed can be used for PV VG-4L design optimisation and also to simulate the performance of PV VG-4L under various conditions. At building efficiency level, the PV VG-4L not only can produce power, but it also has high insulating properties. The promising U-value implies its range of potential applications which can be improved depending on the energy needs and applications, such as for BIPV solar façade (PV curtain walling) in commercial buildings, greenhouses, skylight and conservatory.

Introduction

Leading Beneficiary: SOLIMPEKS

Participants: University of Nottingham (UNOTT)

Task description:

The work package involves fabricating and testing the key components and assembling the components into complete prototypes of technologies. The technologies will be tested in the lab to assess their performance under the nominal set conditions. The testing results will be used to modify and improve the design of the final prototypes, if necessary, which will be used in WP6 (field tests). The availability of this prototype system for field trials will be milestone 3. UNOTT is the work package leader.

Task 4.1: Produce technologies for energy efficient envelope renovation (UNOTT, M7-M17). The components and innovative technologies will be produced after determining their sizes for renovation of different types of building in WP 2. The production of these technologies will be undertaken by different participants of the project Consortium; each participant is assigned to produce one package of technologies according to its expertise in collaboration with other participants.

• SOLIMPEKS will construct PV vacuum glazing as a type of high performance window for electricity generation, light transmission and thermal insulation. PV Vacuum glazing windows will have a U-value below 1 W/m2K for renovation. In addition to creating a simple vacuum within the casing as in conventional practice, different low-cost manufacturing methods and different types of supporting pillars will be investigated such as aerogel. SOLIMPEKS will also produce novel solar thermal and PV systems for integration into buildings. Advanced evacuated tube solar collectors will be investigated where the absorber is treated with a selective Tinox coating to maximise the solar energy absorbed and minimise heat loss through radiation. Novel (poly exchanger for) solar collectors which could form a component of roofing and facade structure will also be produced by this partner together with UNOTT for heating hot water and as a heat source for heat recovery or solar powered cooling. In addition, research will be carried out to combine solar collectors with a heat pump as a renovation solution to existing buildings and to integrate high performance thin-film PV glued straight onto the roof and monocrystalline PV modules into building envelope.

This deliverable concerns the development of the experimental work related with the PV Vacuum glazing.

1 Summary

In recent years, researchers have shown interest in the study of vacuum glazing technology. Innovative designs were developed and researched. Among them are; Bao, Liu [1] who have introduced a novel hybrid vacuum/triple glazing system in which a vacuum glazing unit is enclosed by two glass panels to form a triple glazing unit system. To eliminate additional loads due to pressure difference which can cause unwanted breakage, they designed an equalized air pressure arrangement on both sides of the vacuum glazing unit. Fang, Hyde [2] have performed simulation model using a finite volume model on thermal performance of triple vacuum glazing (TVG) sealed using indium alloy, and 4 mm thick glass panes. In their validated computer simulation work, the emissivity values of the glass sheets were varied from 0.18 to 0.03. The simulated centre U-values are reduced from 0.41 Wm-2K-1 to 0.22 Wm-2K-1 for a 0.4 m by 0.4 m size triple vacuum glazing. Memon [3] introduced a triple vacuum glazing using Cerasolzer CS186 alloy as the edge sealant. From the 3D finite element model, the centre of glass U-value of 0.33 Wm-2K-1 is found achievable. Memon and Eames [4] investigated the building heating performance when retrofitted with the composite edge sealed triple vacuum glazing. An annual space-heating energy savings of 14.58% and 15.31% are expected to be achieved. Meanwhile, if single glazing windows are to be replaced with the designed triple vacuum glazing, a heat loss reduction of 12.92% and 2.69% are achievable. Research on vacuum glazing technology has also led to integrating the technology with other advanced glazing technology. Fang and Hyde [5] have introduced an integration between electrochromic (EC) with vacuum glazing (VG) technology. The EC component was arranged facing the outdoor environment. For an incident solar radiation of 300 W m−2, simulations show that the EC layer is opaque, and the inside temperature of the glass pane is higher than the indoor temperature. Meanwhile, for solar radiation of 1000 W m-2, the outdoor glass pane temperature exceeds the indoor glass pane temperature, of which as a consequence heat is transferred from outdoors to indoors. Ghosh, and Norton [6] integrated suspended particle device (SPD) with vacuum glazing. In their study, a strong correlation between the measures of the clearness of the atmosphere or clearness index was evaluated for south facing vertical glazing. For clearness index below 0.5, the SPD-vacuum glazing transmission was 17% and 1.1% for transparent and opaque states respectively. A group of researchers from China [7] proposed an integration between a thin film PV glazing with a vacuum glazing. The glazing prototype was designed and manufactured in such a way that a lamination layer was sandwiched between the thin film PV glazing unit and a vacuum glazing unit, both are independently manufactured. According to the researchers, although semi-transparent photovoltaic windows can generate electricity in situ, they also increase the cooling load of buildings significantly due to the waste heat as a by-product. Experiment has been conducted and the results have indicated that the prototype can not only generate electricity, but also help reduce the cooling load as well as improve the indoor thermal comfort. Recently,

researchers Ghosh and Sundaram [8] investigated a combined semi-transparent multi-crystalline PV vacuum glazing. In their research, both thermal and electrical performance have been investigated. They have found that the combination of multi-crystalline PV cells with vacuum glazing provide low overall heat transfer coefficient, reduces solar heat gain, generates clean electricity and allows comfortable daylight. This research introduces two designs of thin film PV glazing combined with a vacuum glazing. The novelty of the glazing lies in the designs, manufacturing and application of the PV VG-4L. The heat transfer analysis based on the analytical analysis is discussed and solved numerically in MATLAB. In this report, experimental works are presented, and the model was then validated against indoor and outdoor experimental results.

2 Design concept and heat transfer analysis of thin film PV vacuum insulated glazing (PV VG-4L)

The design of PV VG-4L is illustrated in Figure 1a. PV VG-4L involves an integration between a thin film PV glazing with a double vacuum glazing (both manufactured independently) and an additional layer of self-cleaning coated glass which totalling 4 layers of glass units which gives the total thickness of 14 mm. The layers were combined together via Ethylene Vinyl Acetate (EVA) film using an autoclave facility set at its optimum temperature and pressure.

The thermal resistance network for the PV VG-4L is shown in Figure 1b. Both the width and the length of the PV VG-4L have the same length and denoted as *W*. The heat transfer was analysed based on the following temperature nodes which are; the average glass temperature facing indoors denoted by Tg_1, the average internal glass temperature denoted by Tg_2, the average temperature of the thin film PV glazing denoted by T_{TF} and the average temperature of the self-cleaning coated glass denoted by Tg_4. The lateral heat transfer ends at the point right at the edge sealing and the temperature was denoted as T_{edge1}. Due to high thermal conductivity of the edge sealing, it acts as a short circuit for the heat transfer at the edges of the glazing. Meanwhile, due to high thermal conductivity between *g2* and *g4,* the lateral heat conduction in the glass slab *g2* and thin film PV glazing (*TF)* are assumed negligible. The temperature of the position in *g4,* of which the edge heat transfer takes place is denoted as T_{edge2}. For the uninsulated edges, there will be heat transferred from the internal ambient to the area around the edges.

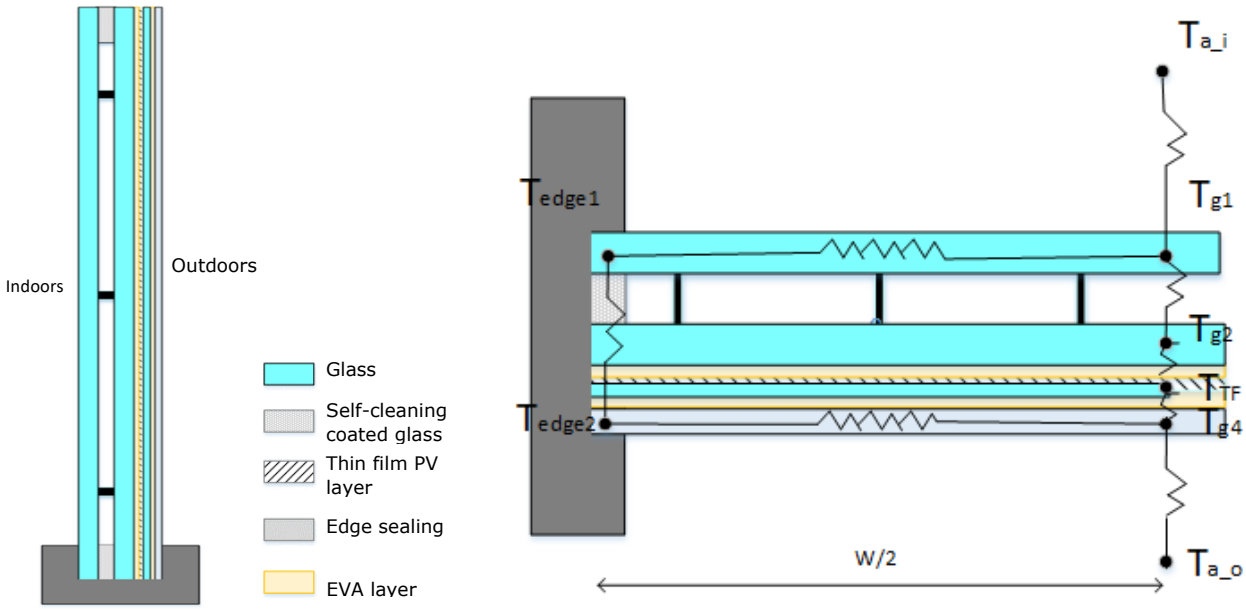

Figure 1: a) Schematics of PV VG-4L and b) the thermal resistance network

The thermal resistance network implies that, at certain level of solar radiation and ambient temperature, the internal surface temperature is in general lower than the external surface temperature. This can be explained as follows. When the PV panel absorbed solar radiation, a fraction of the absorbed solar radiation will be converted into heat meanwhile a fraction will be wasted in the form of heat. This heat released by the PV panel is insulated from the building via the vacuum layer of which, the main heat transfer occurs in the gap are mainly due to radiation and conduction through the support pillars. In the summer, this can be considered as an advantage since the installation of PV glazing would normally cause additional heating during summer of which in return, increase the cooling load of the building. Based on the thermal nodal networks, the energy balance equations were developed. In order to simplify the analysis, the following assumptions have been made:

1) The heat transfer involved is assumed symmetrical. Therefore, we only consider a quarter of the PV VG-4L area in the heat transfer analysis.
2) In this study we have considered the lateral heat transfer through the glass slab in g1. This is due to the fact that, the vacuum glazing is highly thermally insulated which makes the lateral heat transfer to become prominent.
3) The edge boundaries of the PV VG-4L are well insulated and hence the edge losses are assumed negligible.
4) Due to high thermal conductivity of the edge sealing, the edge seal is assumed as a thermal short circuit.
5) Meanwhile, due to high thermal conductivity between *g2* and *g4*, the lateral heat conduction in the glass slab *g2* and thin film PV glazing (*TF*) are assumed negligible.

To simulate the performance of the PV VG-4L, the following energy balance equations were developed for each of the temperature nodes.

For g1:

$$\underbrace{G_{rad}\tau_{TF}\tau_{g5}\tau_{g3}\tau_{g2}\,\alpha_{g1}}_{1} + \underbrace{h_{a\_g1}\left(T_{a\_i} - T_{g1}\right)}_{2} = \underbrace{h_{g1\_g2}\left(T_{g1} - T_{g2}\right)}_{3} + \underbrace{\frac{4\,k_{edge}\delta_{edge}}{\left(\frac{W}{2}\right)^2}\left(T_{g1} - T_{edge1}\right)}_{4} \quad (1)$$

The heat transfer terms are defined as follows:

1: The rate of the solar energy received by the glass cover or surface facing indoors after transmission through different glass layers per unit area; 2: The rate of heat transfer from the indoor ambient to g1 per unit area; 3: The rate of heat transfer from g1 to g2 per unit area. The heat transfer includes heat conduction through the glass slabs of g1, which then followed by heat transfer in the vacuum gap which are due to the heat conduction of the gas particles, heat transfer via radiation and heat conduction through the support pillars, and then followed by heat conduction through the glass slab g4.; 4: The rate of lateral heat

conducted along the x- direction and y-direction of the PV VG-4L from the centre of the PV VG-4L.

(2)

For edge1:

$$\underbrace{\frac{4\,k_{edge}\delta_{edge}}{\left(\frac{W}{2}\right)^2}\left(T_{g1}-T_{edge1}\right)}_{4}+\underbrace{h_{iedge}\gamma_{edge}\left(T_{a\_i}-T_{edge1}\right)}_{5}=\underbrace{h_{edge}\gamma_{edge}\left(T_{edge1}-T_{edge2}\right)}_{6}$$

The heat transfer terms are defined as follows:

5: The rate of heat transfer from the indoor ambient to the edge area per unit glazing area (if not insulated); 6: The rate of heat transfer from edge 1 to edge 2 through *g2, TF* and *EVA* layer per unit area.

For g2:

$$\underbrace{h_{g1\_g2}\left(T_{g1}-T_{g2}\right)}_{3}+\underbrace{G_{rad}\tau_{TF}\tau_{g4}\alpha_{g2}}_{7}=\underbrace{h_{g2\_TF}\left(T_{g2}-T_{TF}\right)}_{8} \quad (3)$$

The heat transfer terms are defined as follows:

7: The rate of the solar energy received by g2 after transmission through different glass layers per unit area; 8: The rate of heat transfer from g2 to TF through the EVA layer per unit area.

For TF:

$$\underbrace{h_{g2\_TF}\left(T_{g2}-T_{TF}\right)}_{8}+\underbrace{G_{rad}\tau_{g4}\alpha_{gTF}}_{9}=\underbrace{h_{TF\_g4}\left(T_{TF}-T_{g4}\right)}_{10} \quad (4)$$

The heat transfer terms are defined as follows:

9: The rate of the solar energy received by *g2* after transmission through different glass layers per unit area; 10: The rate of heat transfer from *TF* .to *g4* through the *EVA* layer per unit area.

For Tedge2:

$$\underbrace{h_{edge}\gamma_{edge}\left(T_{edge1}-T_{edge2}\right)}_{6}=\underbrace{\frac{4\,k_{edge}\delta_{edge}}{\left(\frac{W}{2}\right)^2}\left(T_{edge2}-T_{g4}\right)}_{11} \quad (5)$$

The heat transfer terms are defined as follows:

11: The rate of lateral heat conducted along the x- direction and y-direction of the PV VG-4L from the centre of the PV VG-4L.

For g4:

$$\underbrace{h_{TF\_g4}(T_{TF}-T_{g4})}_{10}+\underbrace{\frac{4\,k_{edge}\delta_{edge}}{\left(\frac{W}{2}\right)^2}(T_{edge2}-T_{g4})}_{11}\underbrace{+G_{rad}\alpha_{g4}}_{12}=\underbrace{h_o(T_{g4}-T_{a\_o})}_{5} \quad (6)$$

The heat transfer terms are defined as follows:

12: The rate of the solar energy received by *g2* after transmission through different glass layers per unit area; 14: The rate of heat transfer from *g4* to T_{a_o} per unit area

The thin film PV VG-4L introduced in this study is new and has never been discussed in existing research. Therefore, in order to theoretically predict the glazing's electrical performance, the equation that has been widely used in the study of PV/Thermal solar collector is utilized. The following correlation developed by Schott [9] and Evans [10] is the most common correlation implemented by researches who study the PV/T –type solar collector such as Sarhaddi, Farahat [11] and Tonui and Tripanagnostopoulos [12]:

$$\eta_{eff}=\eta_{Tref}\left(1-\beta_{ref}(T_{TF}-T_{ref})\right) \quad (15)$$

Where $\beta_{ref}\ is$ the temperature coefficient of the thin film PV cells and η_{Tref} is the electrical efficiency at reference temperature (25˚C). In this study, by referring to [13], for µC-Si/a-Si thin film PV layer, the value of $\beta_{ref}\ is$ -0.36 %, meanwhile, the η_{Tref} is between 1.5 to 4 % depending on the solar radiation by referring to the preliminary experimental results conducted by the current authors.

From the simulation, the values of the average temperature of the glass sheets (layers) were used to compute the heat transfer coefficients summarised in Table 1. By referring to figure 1b the centre thermal resistance R_{centre} and the edge thermal resistance R_{edge} can be computed as in equation (16) and (17) respectively.

$$R_{centre}=\frac{1}{h_{a_{g1}}}+\frac{1}{h_{g1_{g2}}}+\frac{1}{h_{g2_{TF}}}+\frac{1}{h_{TF_{g4}}}+\frac{1}{h_o} \quad (16)$$

$$R_{edge\_tot}=\frac{1}{h_{edge}}+\frac{1}{h_{k\_edge}}+\frac{1}{h_{iedge}} \quad (17)$$

Hence, the centre U-value (U_{centre}) and the total U-value (U_{total})may be computed using equation 18 and 19 respectively:

$$U_{centre} = \frac{1}{R_{centre}} \tag{18}$$

$$U_{total} = U_{centre+}U_{edge\_tot} \tag{19}$$

In this study, to solve the energy balance equation, we have used the inverse matrix method. MATLAB is used to carry out the iteration process with Newton-Raphson iteration technique is used to estimate the temperature and hence the temperature-dependant heat transfer coefficients of the variables.

Table 1: the definition of the symbol used

Symbol	Definition	Symbol	Definition
α	Solar absorptance	τ	The solar transmittance
γ_{edge}	Correction factor due to the total area of edge sealing	γ_p	Correction factor due to the total area of the support pillars
δ_{edge}	The edge sealing thickness	G_{rad}	Total global solar radiation incident upon the glazing structure.
h_P	Heat transfer coefficient through the support pillars	h_{edge}	Conductive heat transfer coefficient due to the edge sealing
h_{k_edge}	The lateral heat transfer to the glass edge	h_{iedge}	Total heat transfer coefficient from the indoor ambient air to the uninsulated edge sealing area
h_{a_g1}	Total heat transfer coefficient from the internal ambient to g1	h_{g1_g2}	The total heat transfer coefficient from g1 to g2 of vacuum glazing
h_{TF_g4}	The total heat transfer coefficient by conduction from the thin film PV glazing layer *TF* to *g4.*	h_{g2_TF}	The total coefficient of heat transfer by conduction from *g2* to the thin film PV glazing layer *TF.*
h_o	Total heat transfer coefficient from the external glass *g4* to the ambient	k_{edge}	Thermal conductivity through the edge sealing
T_{a_o}	Outdoor ambient temperature	T_{a_i}	Indoor ambient temperature

3 Experimental validation of the theoretical model

3.1 U-value measurement using a TEC driven calibrated hot box

A PV VG-4L prototype using an amorphous silicon (α-Si) solar cell as shown in Figure 2 was manufactured. The U-value of the prototype was evaluated using the TEC-driven calibrated hot box built at the University of Nottingham. Interested readers may refer to [14] for further details. As can be seen in Figure 3, by following closely ISO 12567 standards, the sample was installed at the specimen area of the calibrated hot box. It was tested under three different air temperature conditions summarised in Table 2. However, the air speed in the hot and cold side were fixed at 0.3 m/s and 1.5 m/s respectively. Using the calibrated hot box, we could estimate the total heat transfer coefficient from the hot and cold surface of the PV VG-4L prototype. The values were then used as the input parameters for the computer simulation. To derive the absolute error, the Kline–McClintock second power law as given in NCEES (National Council of Examiners for Engineering and Surveying) (2001) is used. These errors were represented by the error bars of the associated curves. Additionally, the guideline in ISO 12567 was also being referred to evaluate the error from indoor testing.

Figure 2: The PV VG-4L prototype

The mathematical model validation method is performed by comparing the results obtained experimentally and theoretically based on the trends shown on the related graphs. In this study, the mathematical model has been validated against the indoor experimental data with the input parameters recorded in the experiment were used in the computer simulation for all the three different conditions. In addition to the direct comparison between the simulation and theoretical curves, the validation of the mathematical model is further justified using root mean square percentage deviation (RMSPD). As shown in Figure 4, and summarised in Table 3, the evaluated glazing surface temperatures and U-value are found to be in good agreement such

that the trend of the theoretical curves are consistent with the experimental curves and the computed RMSPD for the temperatures and U-value are 4.02% and 0.92% respectively.

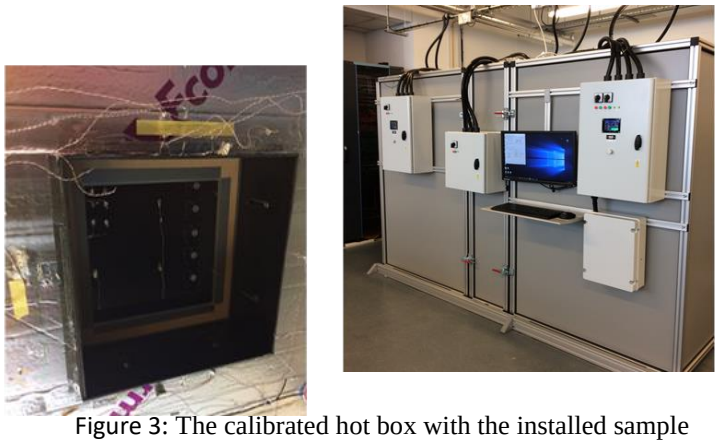

Figure 3: The calibrated hot box with the installed sample

Table 2: Comparison between the Theoretical and Experimental Results for the glazing surface temperature and U-value using the calibrated hot box under different sets of controlled ambient temperature conditions

Cond.	Text (˚C)	Tint (˚C)	Tint (Exp) (˚C)	Text (Exp) (˚C)	Tint (Theo) (˚C)	Text (Theo) (˚C)	U-value total (Exp)	U-value total (Theo)
1	12.7	32.70	30.34	13.50	29.90	13.37	0.56	0.57
2	17.5	27.5	27.40	18.65	26.42	17.84	0.57	0.57
3	7.6	27.83	25.19	9.13	25.67	8.29	0.56	0.56

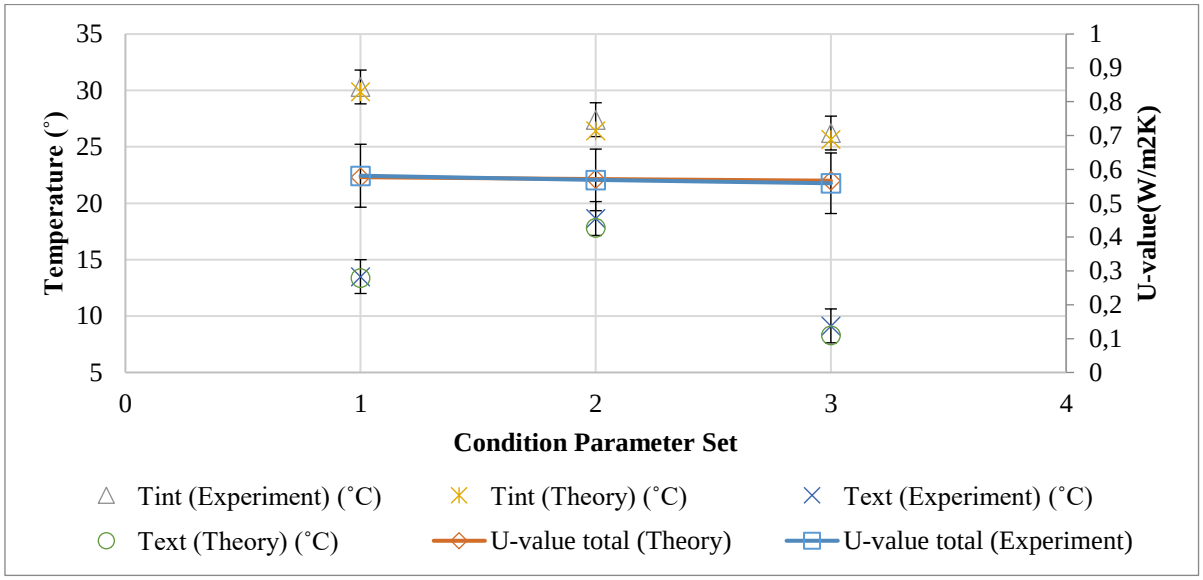

Figure 4: Comparison between the theoretical and experimental results for the glazing surface temperature and U-value using the calibrated hot box.

3.2 Performance analysis under real conditions.

The developed mathematical model has been validated against indoor experimental analysis. Nonetheless, the true performance of the PV VG-4L under real sky conditions still needs to be investigated in order to further justify the validity of the mathematical model especially that the electrical performance of the thin film PV glazing could not be evaluated indoors. That said, this section first discusses the performance of the PV VG-4L under real conditions. To carry out the testing, the prototype was installed at E.ON 2016 research house at the University of Nottingham, United Kingdom with latitude of 52.9438° N, and longitude of 1.1934° W. It is worth emphasising that the outdoor monitoring of the PV VG-4L has been conducted under two conditions; during the day and during the night (at zero solar radiation). The thermal and electrical characteristics of the PV VG-4L under real conditions were monitored using the sensors as summarised in Table 3. During the day, the reading given by the heat flux sensor for the thermal transmittance of the PV VG-4L is not reliable due to the error from the solar radiation to the heat flux sensor and also due to the absorbed solar radiation by the PV layer. Therefore, during the day, the only parameters that are being considered are the surface temperature difference of the PV VG-4L and its electrical power produced. The typical monitoring period is between 9:30 a.m. to 6:00 p.m. in a typical day of May and June. Meanwhile, the focus of the experiment during the night is the thermal transmittance measurement or U-value. A 1kW radiator was used as the heat source for indoors.

Table 3: Measured parameters and uncertainties

Parameters	Sensor	Uncertainties
Temperatures	K-type Thermocouples	± 1.5 ˚C

Heat flux	Hukesflux Thermal Sensors	± 1.9 x 10^{-6} V/(W/m^2)
Solar radiation	Pyranometer	±5%
Maximum power produced by the PV VG-4L	RO4 with Keysight 34972A	Electric current (I) (±1.5 µA) Voltage (V) (± 190 µV)

Figure 5 shows the solar radiation, surface temperatures of the PV VG-4L, and both internal and external; glazing surface temperature during the day and night. It should be noted that for the data taken on the 23rd to 24th of May 2021 the internal heat source was switched off during the day meanwhile, the average heating temperature was set at 30 ˚C during the night (i.e. from 8 p.m. to 4 a.m. the next day) to heat the ambient room at 24 to 25 ˚C. On the day of testing, the sky was in a clear sky condition and hence clear pattern of solar radiation curve with the time of the day was obtained. Another set of experiment was conducted to evaluate the performance of the PV VG-4L on the 20th to 21st of June 2021. However, as can be seen on Figure 6, during the day of testing, the sky turned cloudy and hence periods of fluctuating solar radiation were recorded. During the aforementioned period, steady state condition of the PV VG cannot be well justified. This is attributed to the response time of the glass (time constant) which is caused by the thermal mass of the PV VG components. Furthermore, the influence of the thermal time response of the PV VG to the sudden drop in solar radiation is clearly shown by the change in the recorded temperature profiles from 1:45 p.m. to 2:15 p.m. During the aforementioned period, the average intensity of the incident solar radiation dropped for a step change from 400 W/m² to 60 W/m2 and the temperature profiles clearly follows an exponential decay lagging behind the step change. Additionally, by carefully examining Figure 6, at points in which there was a sudden drop in the value of solar radiation due to the movement of clouds, the temperature profiles are also observed to lag behind the values of solar radiation.

It is worth noting that, in both graphs, at low–zero solar radiation, the indoor surface temperature of the PV VG-4L is in general higher than its external surface temperature. However, as the incident solar radiation increases, the external surface temperature increases. The trend of the graph is explained as follows; when the PV component of the PV VG-4L absorbed the incident solar radiation, a fraction was converted into electrical energy meanwhile the rest was wasted in the form of heat. However, the vacuum layer behind the PV component of the PV VG-4L act as the insulation layer or barrier to the wasted heat from being transferred indoors. As a result, the external surface temperature of the PV VG-4L became higher compared to its internal surface temperature. In the summer, this will be an advantage in comparison to the typical installation of BIPV in double glazed configuration. For the data analysis, the temperatures, solar radiation and heat flux were recorded for every 1 s meanwhile, the electrical parameters were recorded for every 10 s.

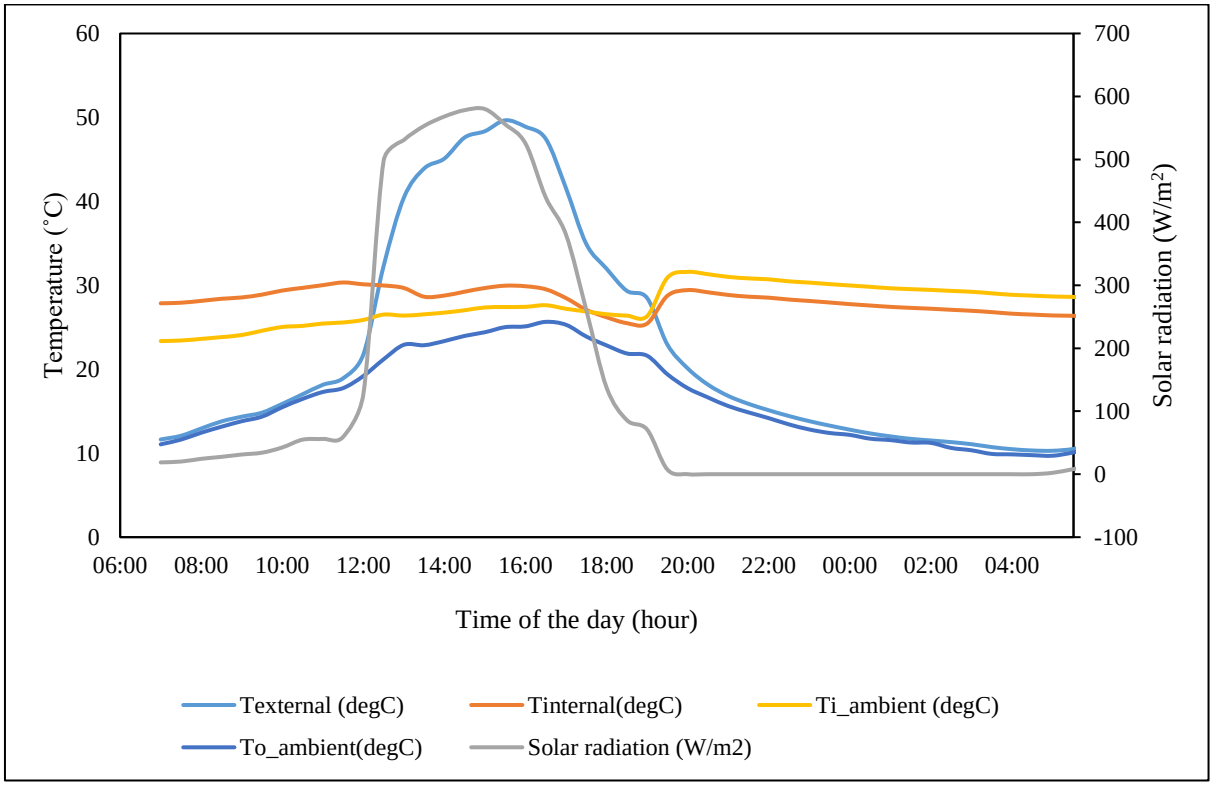

Figure 5: Variation in the external glazing surface temperature (Texternal), internal glazing surface temperature (Tinternal), Outdoor ambient temperature (To_ambient), indoor ambient temperature (Ti_ambient) and solar radiation with time of the day (23rd of May (7:00 a.m). to 24th of May 2019 (4:00 a.m.))

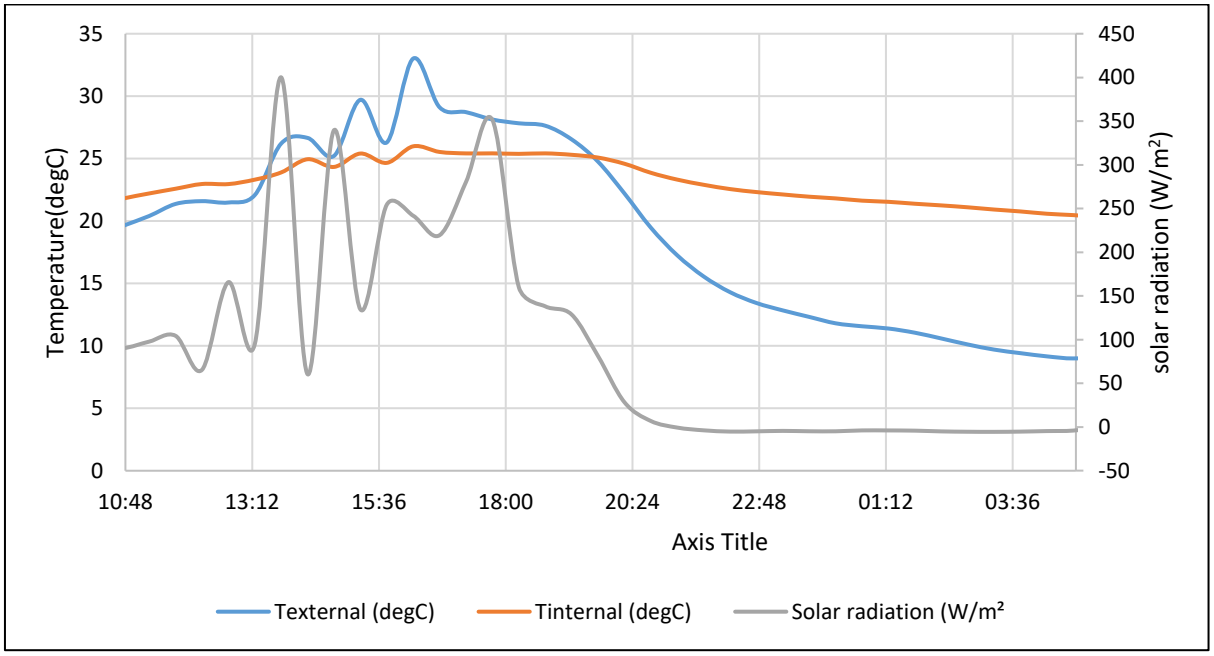

Figure 6: Variation in the external glazing surface temperature (Texternal), internal glazing surface temperature (Tinternal), Outdoor ambient temperature (To_ambient), indoor ambient temperature (Ti_ambient) and solar radiation with time of the day (20th of June from 9:15 a.m. to 21st of June 2019 9:15 a.m.)

The outdoor experimental results obtained from the 23rd to 24th of May, as discussed previously, were compared with the theoretical results using the developed mathematical model. Due to the varying condition of the ambient climate, the electrical performance and thermal characteristics of PV VG-4L in a steady state condition are analysed as per time constant of the PV VG-4L. From our analysis, it is concluded that the computed time constant for the PV VG-4L is approximately 30 minutes. The experimental results were compared based on the PV VG-4L surface temperature difference and electrical performance at quasi-steady state during the day and thermal transmittance or U-value during the night. Based on local weather data, the average wind speed during the day and night were approximated at 4.5 m/s and 3.5 m/s respectively. The comparisons between the outdoor experimental and theoretical results are represented in Figure 7 and Figure 8 for the reading during the day and night respectively. The trend given by both outdoor experimental and theoretical curves are in good agreement. Figure 6 shows that the maximum power produced at average solar radiation of 600 W/m^2 is approximately 18 W/m^2 for 0.4 m x 0.4 m PV VG-4L made of amorphous silicon solar cells. It is worth emphasizing that, a different power produced is expected when a different type of thin film PV is used as the prototype. For example, using the validated mathematical model, it is predicted that, if amorphous/microcrystalline silicon solar cells at 20% transparency is used as the thin film PV layer, the power output at the same average solar radiation can achieve as high as 32 W/m^2. In order to further justify the validity of the mathematical model, error analysis using RMSPD analysis was performed. The average RMSPD for the glazing surface temperatures, the power produced, and U-value are 2.90 %, 8.7% and 2.89 % respectively. It is worth noting that the derived absolute errors for the power produced are too small to be included in the plotted curves.

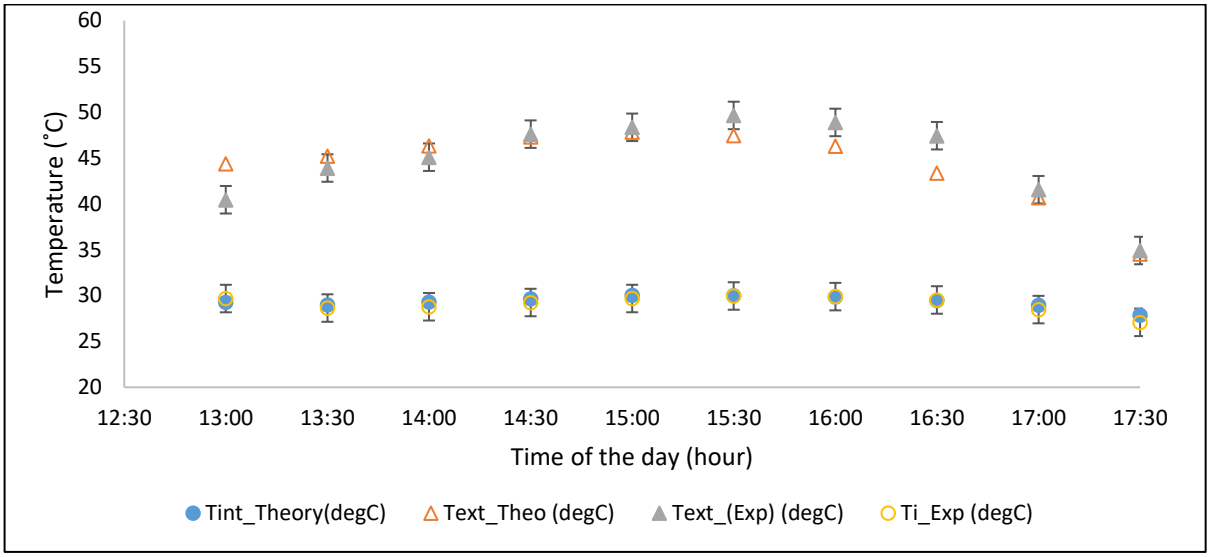

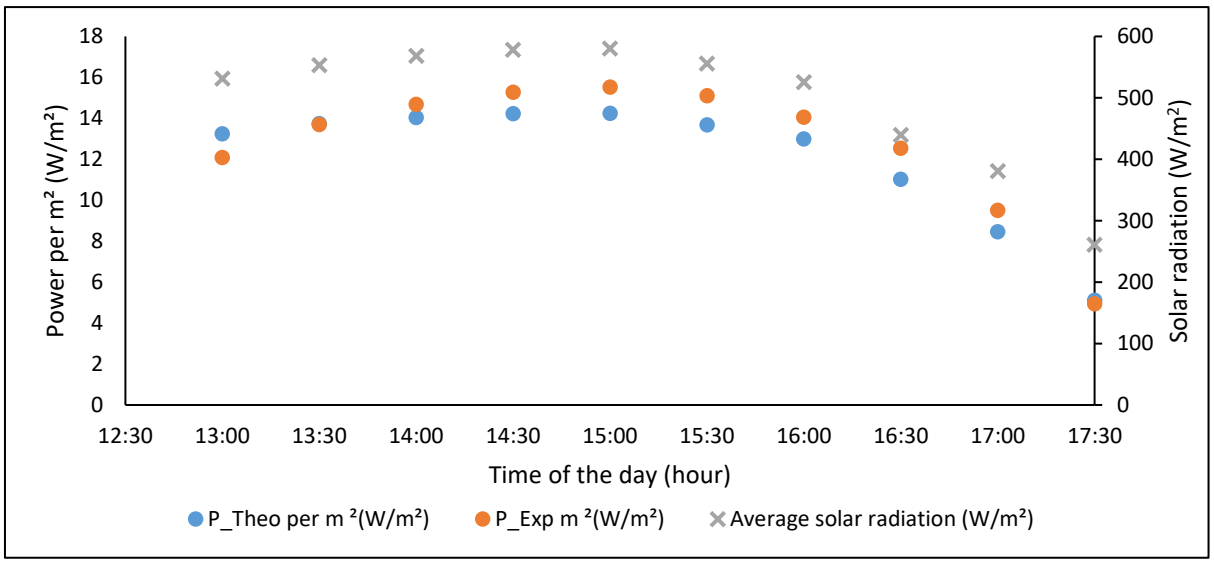

Figure 7: Top: Outdoor Experimental and Theoretical Curves for the Glazing surface temperatures (Tint for the internal surface and Text for the external surface) and bottom: Power produced per m^2 for 0.4 m x 0.4 m prototype as per time constant of the PV VG-4L with time of the day as (data was taken on the 23rd of May 2019 during the day)

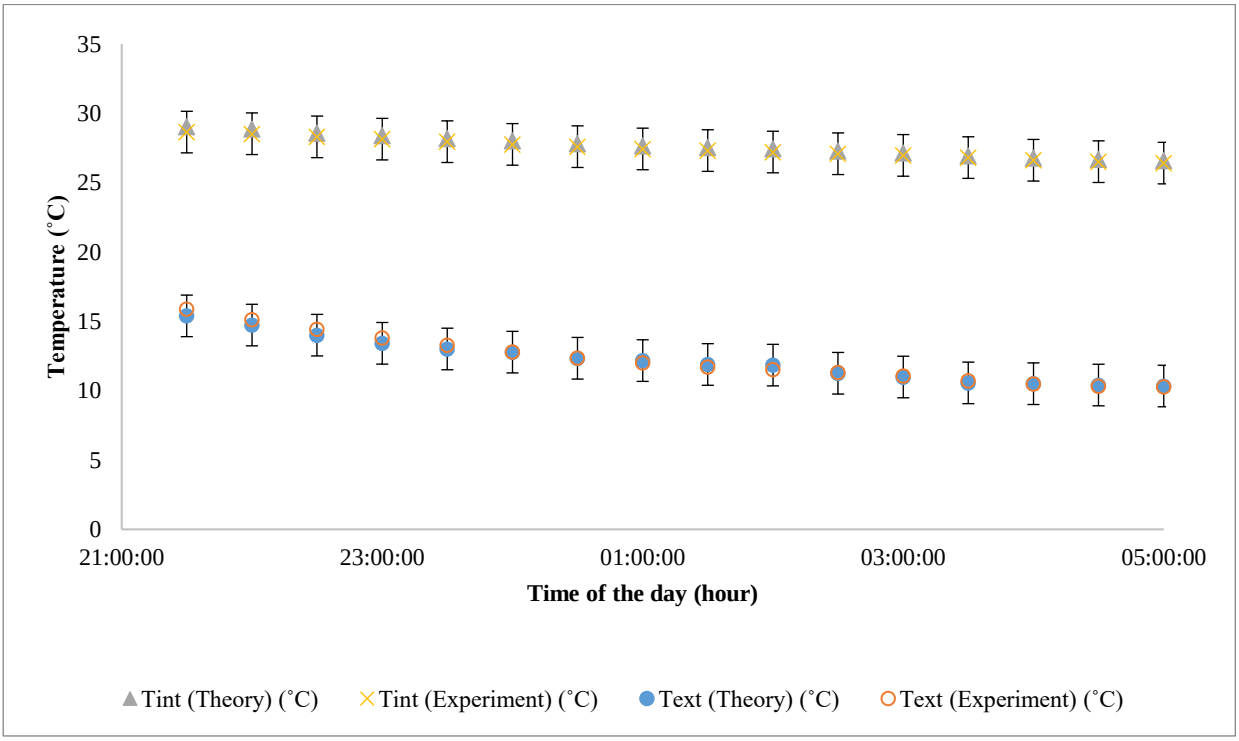

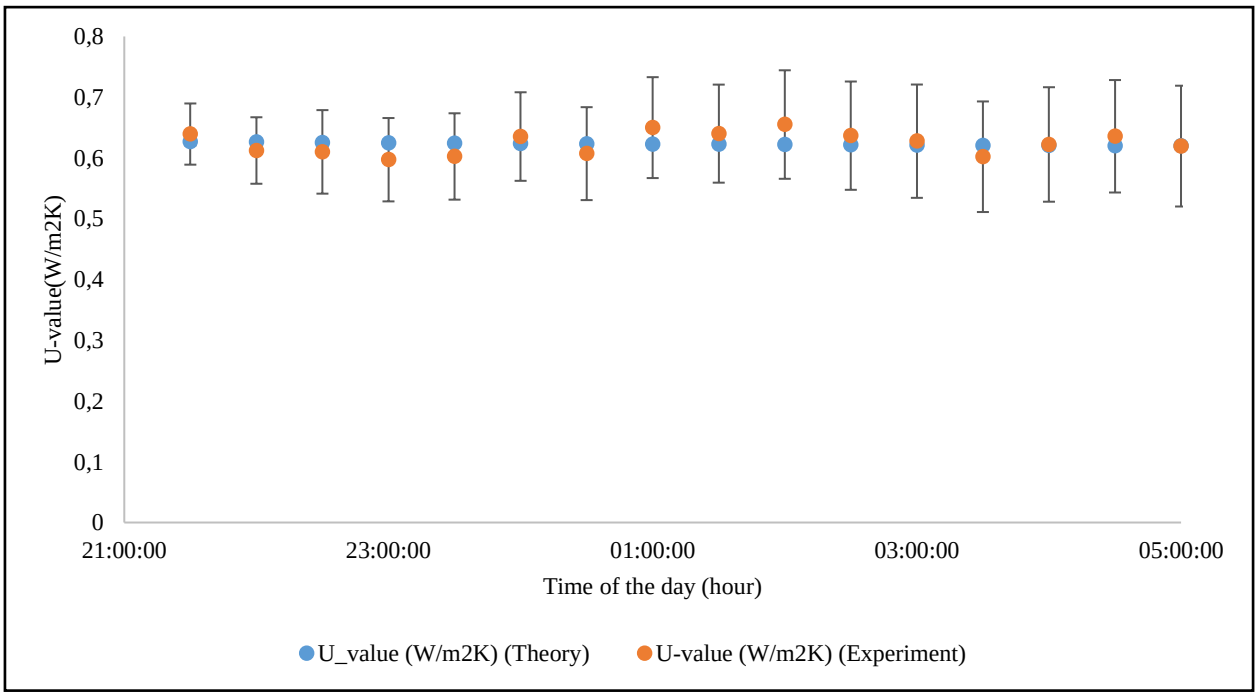

Figure 8: Top: Outdoor Experimental and Theoretical Curves for the Glazing surface temperature and bottom: U-value for 0.4 m x 0.4 m prototype as per time constant of the PV VG-4L with time of the day as (data was taken on the 23rd of May 2021 to 24th of May 2021 at low-zero solar radiation)

Conclusions

An innovative Thin Film Photovoltaic Glazing with Vacuum Insulated Layer (PV VG-4L) is presented in this research. A mathematical model was developed by taking into account all the parameters related to the individual component of a typical vacuum glazing unit which is the dominant in the design and also the fraction the solar radiation absorbed by the different layers of PV VG-4L. To validate the mathematical model, a lab-scale prototype was manufactured and tested indoors using a calibrated hot box, and outdoors by installing the sample at a research house. Under controlled conditions, the overall U-value of the PV VG-4L was measured to be as low as 0.6 W/m2K. When investigated under real conditions, an obvious trend in glazing surface temperature variation with solar radiation was obtained. During low to zero solar radiation, the internal glazing surface temperature is on average higher in comparison to the external glazing surface temperature. However, as the solar radiation increases, the by-product of the absorbed heat by the thin film PV glazing layer, has led to an increase in the external glazing surface temperature as the heat is hindered from being transferred indoors by the vacuum layer. At average solar radiation of 600 W/m2 the PV VG-4L can produced in total of 18 W of power per m2 of panel. Meanwhile, as shown in Figure 7, at low to zero solar radiation (i.e. during the night), at outdoor ambient temperature of 14 ˚C, the average U-value of the typical PV VG-4L was found to be as low as 0.6 W/m2K while maintaining the indoor ambient temperature at 30 ˚C. Please note that high internal ambient temperature was obtained due to the use of heater at its maximum setting. For a conventional thin film PV glazing, to improve the thermal performance of the thin film PV glazing, a combination with a double-glazing unit is possible with the estimated U-value of 2.5-2.8 W/m2K depending on the type of gas used to provide the insulation in the air gap. Clearly, the vacuum layer introduced in the PV VG-4L design presented in this research is better in performance with the slim configuration of the glazing unit as an additional benefit. The results also show that the PV VG-4L not only can produce power but also has high insulation properties when compared to a single thin film PV glazing with a typical U-value of 5 W/m2K; the U-value is higher by almost 90%. The promising U-value implies its range of potential applications can be improved depending on the energy needs and applications, such as for BIPV solar façade (PV curtain walling) in commercial buildings, greenhouses, skylight and conservatory.

References

[1] Bao, M., et al., Novel hybrid vacuum/triple glazing units with pressure equalisation design. Construction and Building Materials, 2014. 73(Supplement C): p. 645-651.

[2] Fang, Y., et al., Enhancing the thermal performance of triple vacuum glazing with low-emittance coatings. Energy and Buildings, 2015. 97(Supplement C): p. 186-195.

[3] Memon, S., Experimental measurement of hermetic edge seal's thermal conductivity for the thermal transmittance prediction of triple vacuum glazing. Case Studies in Thermal Engineering, 2017. 10(Supplement C): p. 169-178.

[4] Memon, S. and P.C. Eames, Predicting the solar energy and space-heating energy performance for solid-wall detached house retrofitted with the composite edge-sealed triple vacuum glazing. Energy Procedia, 2017. 122(Supplement C): p. 565-570.

[5] Fang, Y., et al., Thermal performance analysis of an electrochromic vacuum glazing with low emittance coatings. Solar Energy, 2010. 84(4): p. 516-525.

[6] Ghosh, A., B. Norton, and A. Duffy, Effect of atmospheric transmittance on performance of adaptive SPD-vacuum switchable glazing. Solar Energy Materials and Solar Cells, 2017. 161(Supplement C): p. 424-431.

[7] Zhang, W., L. Lu, and X. Chen, Performance Evaluation of Vacuum Photovoltaic Insulated Glass Unit. Energy Procedia, 2017. 105(Supplement C): p. 322-326.

[8] Ghosh, A., S. Sundaram, and T.K. Mallick, Investigation of thermal and electrical performances of a combined semi-transparent PV-vacuum glazing. Applied Energy, 2018. 228: p. 1591-1600.

[9] Schott, T. Operational temperatures of PV modules. in 6th PV solar energy conference. 1985.

[10] Evans, D., Simplified method for predicting PV array output. Solar Energy, 1981. 27: p. 555–560.

[11] Sarhaddi, F., et al., An improved thermal and electrical model for a solar photovoltaic thermal (PV/T) air collector. Applied Energy, 2010. 87(7): p. 2328-2339.

[12] Tonui, J.K. and Y. Tripanagnostopoulos, Air-cooled PV/T solar collectors with low cost performance improvements. Solar Energy, 2007. 81(4): p. 498-511.

[13] Virtuani, A., D. Pavanello, and G. Friesen, Overview of Temperature Coefficients of Different Thin Film Photovoltaic Technologies. 2010. 4248-4252.

[14] JARIMI, H., et al. An affordable small calibrated hot box suitable for thermal performance measurement of a glazing unit. in 17th International Conference on Sustainable Energy Technologies 21st to 23rd August 2018. 2018. Wuhan, China.